Scripta Materialia 156 (2018) 80–84

Contents lists available at ScienceDirect

Scripta Materialia

journal homepage: www.elsevier.com/locate/scriptamat

Regular article

Exploring radiation induced segregation mechanisms at grain boundaries in equiatomic CoCrFeNiMn high entropy alloy under heavy ion irradiation

Christopher M. Barr [a], James E. Nathaniel II [a], Kinga A. Unocic [b], Junpeng Liu [c], Yong Zhang [c], Yongqiang Wang [d], Mitra L. Taheri [a,*]

[a] Materials Science and Engineering Department, Drexel University, Philadelphia, PA, USA
[b] Materials Science and Technology Division, Oak Ridge National Laboratory, Oak Ridge, TN, USA
[c] State Key Laboratory for Advanced Metals and Materials, University of Science and Technology Beijing, Beijing, China
[d] Center for Integrated Nanotechnology, Los Alamos National Laboratory, Los Alamos, NM, USA

ARTICLE INFO

Article history:
Received 5 June 2018
Accepted 23 June 2018
Available online 20 July 2018

Keywords:
High entropy alloys
Radiation induced segregation
Grain boundaries
Chemical complexity
Radiation damage

ABSTRACT

High entropy alloys have gained significant interest due to several unique properties including enhanced radiation resistance. In this work, radiation induced segregation, a key phenomenon observed in alloys under irradiation, is examined for the first time at high angle grain boundaries under Ni heavy ion irradiation in the CoCrFeNiMn alloy. Our experimental study indicates significant Mn depletion and Co and Ni enrichment at grain boundaries. The segregation is discussed in the context of a proposed vacancy dominated radiation induced segregation mechanism and compared to existing models in conventional single core component alloys including stainless steels.

© 2018 Published by Elsevier Ltd on behalf of Acta Materialia Inc.

Single-phase and multi-phase alloys of multiple core principle elements broadly classified as high entropy alloys (HEAs) have recently garnered extensive interests [1–4] due to numerous improved or unique properties in comparison to conventional alloys. These multi-principle element alloys, for example, have shown excellent room temperature and cryogenic fracture toughness [5], high ductility [6,7], increased corrosion resistance [8], and improved wear properties [9]. Researchers have explored the potential of particular single-phase concentrated solid solution alloys (SP-CSAs) and HEAs for nuclear energy applications by examining their response under irradiation [10–14]. Early experimental and computational studies of SP-CSA such as equiatomic FeNi, CoFeNi, CoCrFeNi, and CoCrFeNiMn under ion and electron irradiation environments have indicated reduced swelling, delayed void formation, slower irradiation induced defect cluster migration, and reduced dislocation size and density in comparison to pure Ni.

The improved radiation response of SP-CSAs have been attributed to proposed compositional complexity and high configurational entropy leading to slower point defect diffusion and delayed defect evolution in comparison to conventional alloys or pure metals [12,15,16]. In addition to the defect evolution during irradiation, two recent studies have explored radiation induced segregation (RIS) at dislocations in SP-CSA alloys. Lu et al. [17] reports that the magnitude of RIS at irradiation induced dislocation loops is minimized in CoCrFeNiMn at 500 °C under 3 MeV Ni^{2+} irradiation conditions. In contrast, He et al. [18] shows notable Co enrichment and Mn depletion with negligible Cr, Fe, Ni segregation at irradiation induced dislocation loops under 1.25 MeV electron irradiation. While these studies provide an early indication of solute segregation under irradiation, to date, no experimental efforts have been undertaken to characterize RIS at grain boundaries (GBs) in the most commonly studied CoCrFeNiMn HEA. Solute segregation to GBs is known to be a key microstructural feature in irradiated assisted stress corrosion cracking and localized intergranular corrosion resistance in several conventional alloys including Fe-Ni-Cr austenitic alloys [19]. Therefore, a fundamental understanding of experimentally observed GB segregation behavior and potential GB RIS mechanisms are critical for possible radiation environment applications.

In this study, we explore GB RIS in CoCrFeNiMn under heavy ion irradiation. The experimental observations indicate substantial segregation of constituent elements at GBs. The solute segregation at 2 and 3 dpa was compared to conventional alloys; we observed significant segregation of Mn, Ni, and Co to random high angle GBs (RHAGBs). The segregation is discussed in the context of a proposed vacancy

* Corresponding author at: Department of Materials Science & Engineering, Drexel University, LeBow Hall 441, 3141 Chestnut Street, Philadelphia, PA 19104, USA.
E-mail address: mtaheri@coe.drexel.edu (M.L. Taheri).

https://doi.org/10.1016/j.scriptamat.2018.06.041
1359-6462/© 2018 Published by Elsevier Ltd on behalf of Acta Materialia Inc.

dominated RIS GB mechanisms in multi-component alloys and compared to conventional single component alloys including commercial and model austenitic Fe- and Ni-based alloys.

Equiatomic CoCrFeNiMn ingots were produced by vacuum induction levitation melting in high purity Ar atmosphere. The samples were further homogenized for 20 h at 1100 °C in Ar atmosphere, followed by straining via a 25% rolling reduction and annealed at 1100 °C for 2 h and water quenched. Fig. 1a illustrates the inverse pole figure colored orientation map of the alloy prior to irradiation which has an average grain size with twin boundaries included of 87 ± 44 μm. Heavy ion irradiations were completed with 3 MeV Ni^{2+} ions to a total fluence of 3×10^{15} at 500 °C (dose rate of 3×10^{-3} dpa/s). The corresponding displacements per atom (dpa) as a function of cross-sectional depth, shown in Fig. 1b, was determined using SRIM-2008 with the quick Kinchin-Pease calculation (40 eV displacement threshold energy for all elements) [20]. Fig. 1b also indicates the estimated level of implanted Ni as a function of cross-sectional depth. RIS was characterized at RHAGBs by Scanning Transmission Electron Microscopy (STEM) – energy dispersive x-ray spectroscopy (EDS) on cross-sectional focused ion beam (FIB) lift-out specimens [21]. All EDS measurements were taken at cross-sectional depths of 0.5 μm and 1 μm which corresponded to approximately 2 and 3 dpa, respectively. STEM-EDS was completed using a FEI F200X Talos S/TEM operated at 200 kV; FIB-prepared samples were approximately 80 nm in thickness while all GBs regions reported were edge-on to the electron beam. In addition to the RIS measurements, STEM-annular dark field (ADF) taken with a JEOL 2100F S/TEM, shown in Fig. 1c, indicates there are no irradiation induced voids at this relatively low to intermediate dose regime. The lack or reduction of void swelling in comparison to Ni and particular Ni binary alloys is consistent with previous literature [10,22–25].

Fig. 2a illustrates the representative RIS microchemistry for the CoCrFeNiMn HEA at 2 dpa. The change in the matrix composition from the GB composition of the five elements is shown in Fig. 2b. At both 2 and 3 dpa there is nearly identical solute segregation behavior at RHAGBs. Substantial Co and Ni enrichment to approximately 27 at.% and Mn depletion to approximately 9 at.% were observed. The level of Cr and Fe at GBs is near the adjacent matrix compositions and within approximately 1 at.% depletion at both 2 and 3 dpa. Supplemental Fig. S1 shows a representative STEM-EDS elemental map collected at a RHAGB. The 3 dpa condition at 1 μm cross-sectional depth as shown in Fig. 1b is near the Ni ion irradiation end of range where the interstitial injected effects can modify the irradiation response [24,26]. In this case, slightly less Co and Ni enrichment and Mn depletion are observed in comparison to the 2 dpa depth. The segregation width of the elemental depletion and enrichment in Fig. 2 is approximately 5 nm on both sides of the GB. The segregation width is consistent with minor STEM-EDS beam broadening effects but is consistent with RIS segregation width in extensively studied austenitic [27,28] and ferritic steels [29,30] under similar 400 °C proton and 500 °C heavy ion irradiations.

The results presented above are the first reported analyses of GB RIS in CoCrFeNiMn. The experimental data can be compared to preceding studies that have explored dislocation RIS in the same alloy. Segregation profiles measured by STEM-EELS across edge-on dislocations in Lu et al. [17] indicate no clear solute segregation in CoCrFeNiMn irradiated to 38 dpa at 500 °C using 3 MeV Ni^{2+} heavy ions. Lu et al. [17] attribute the reduced and minimal dislocation RIS to high lattice distortion which they propose enhances vacancy/interstitial recombination and subsequently suppress the overall defect fluxes to point defect sinks. In the same HEA, He et al. [18] observed significant Mn depletion, Co enrichment, and no detectable segregation of Ni, Cr, or Fe at Frank partial dislocations at 1 dpa under 1.25 MeV electron irradiation at 400 °C using STEM-EDS. In their study, they attribute the observed segregation behavior in this and other compositionally complex HEA alloys through an interstitial binding mechanism [31] and associated atomic size difference. The smaller Co and Ni atomic size in comparison to larger Fe and Cr atoms are favored for preferentially coupling with interstitials and subsequently enrich at dislocations. The proposed dislocation solute segregation mechanism does not include vacancy-defect preferential interactions. While these two studies offer distinct perspective and varying observations of chemical segregation to dislocations under irradiation in CoCrFeNiMn, the mechanism for RIS at GBs have not been previously explored. Furthermore, while comparison to the existing dislocation RIS studies are valuable due to the limited existing studies, the overall segregation mechanism and sink strength can be quite different than GBs [32]. Specifically, dislocations, in comparison to a random general GB, are a biased defect for interstitials and so it is possible that the dominant solute segregation mechanisms of the core elements can differ.

As described above, there are very limited experimental segregation studies under irradiation in fcc based compositional complex alloys such as HEAs. However, there has been substantial effort over the past several decades to have a mechanistic understanding of irradiation induced GB segregation in conventional (i.e. single core element) Fe- and Ni-based fcc based commercial and model alloy systems such as 304 and 316 stainless steels. The modified inverse Kirkendall (MIK) model [33,34] has been successfully implemented to predict RIS trends in both model and commercial austenitic Fe-Ni-Cr alloys. The MIK model was built on the foundation of the Perks model [35] where RIS is dictated by differences in species dependent atomic-vacancy jump rates (i.e. inverse Kirkendall effect mechanism). The MIK model added to the Perks model by incorporating additional terms to account for localized short-range ordering and alloy composition. Importantly, both models rely exclusively on the coupling of the solute flux with the vacancy flux and make note that interstitial effects are not required to sufficiently describe the RIS behavior of the key core and alloying elements: Fe, Ni, and Cr. More recently, Yang et al. [36] and others [37–40] have indicated that incorporation of preferential atom-interstitial coupling via an interstitial binding mechanisms [31] can

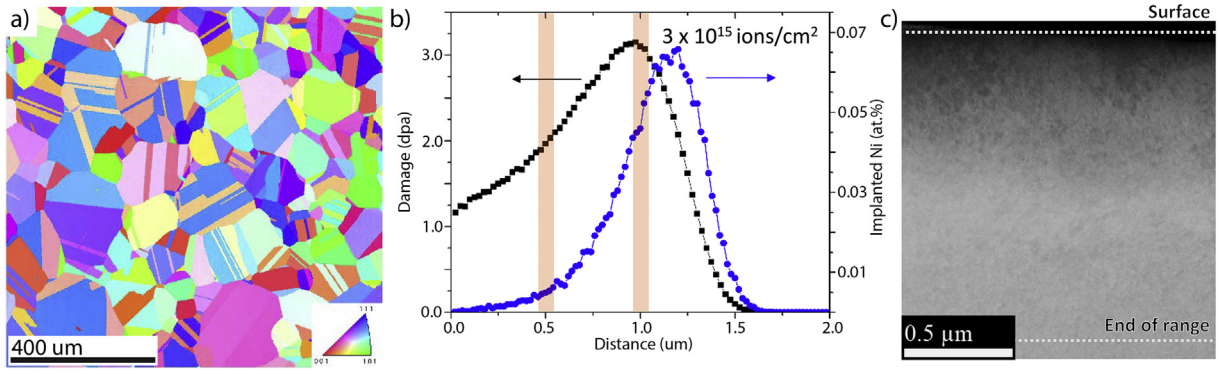

Fig. 1. (a) Inverse pole figure colored map of the coarse grain CoCrFeNiMn used for the ion irradiation; (b) SRIM calculated dpa as function of cross-sectional depth for 3 MeV Ni^{2+} irradiations; (c) STEM-ADF image of irradiated sample with implanted Ni end of range and surface highlighted.

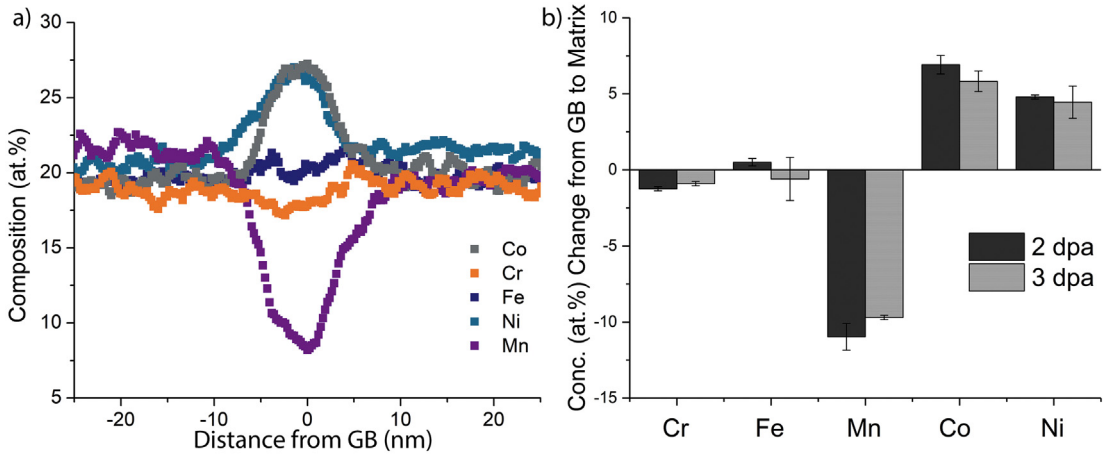

Fig. 2. (a) Representative radiation induced segregation profile at a random high angle GB at 2 dpa; (b) Change in GB to matrix composition at both 2 and 3 dpa for the CoCrFeNiMn HEA indicating significant Mn depletion and Ni and Co enrichment.

provide even closer agreement between modelled and experimentally observed RIS in Fe-Ni-Cr and Ni-Cr model alloys. However, incorporation of the preferential atom-interstitial coupling requires careful assessment of ab-initio first principle calculations of interstitial-atom binding energies and/or experimentally derived values. For comparing generalized trends in RIS between conventional and compositionally complex HEA alloys, we consider RIS to be exclusively vacancy dominated in similar fashion to the original Perks and MIK models for Fe-Ni-Cr. As detailed in the description of the MIK model [34], the flux of a particular element is a function of the local concentration and species dependent vacancy diffusivity. Vacancy diffusivities in the MIK model are related to thermal, high temperature vacancy self-diffusion coefficients in Fe-Ni-Cr [41]. Assuming that interstitial contributions are set equal for all elements, the ability to determine if the major elements enrich or deplete is related to the relative diffusivities: d_{Cr}/d_{Ni}, d_{Fe}/d_{Ni}, and d_{Cr}/d_{Fe} in Fe-Ni-Cr. Therefore, the fastest vacancy diffuser element will deplete while the slowest vacancy diffuser will enrich at the point defect sink. Fig. 3 shows the temperature dependent diffusivities ratios in Fe-20Cr-15Ni [41] where $d_{Cr}/d_{Ni} > d_{Fe}/d_{Ni} > 1$. As is now well established with extensive experimental research, this leads to Cr depletion and Ni enrichment in Fe-Ni-Cr alloys under high temperature irradiation.

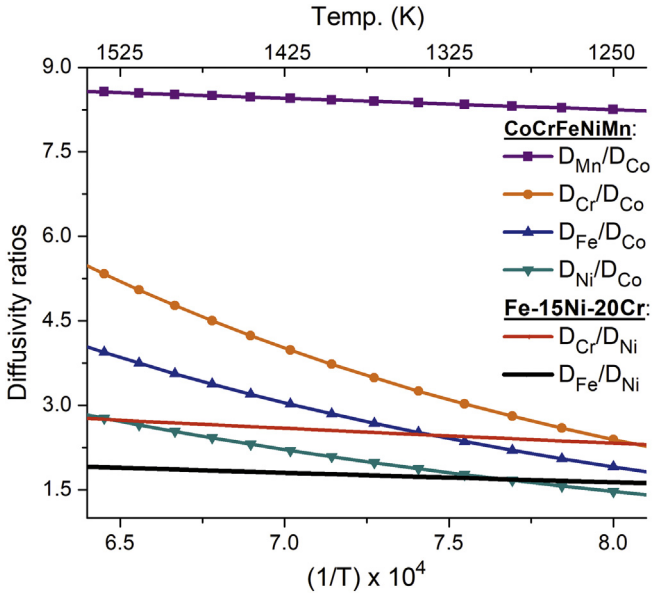

Fig. 3. Thermal diffusivity ratios as a function of temperature for the various elements in Fe-20Cr-10Ni [41] and CoCrFeNiMn [42].

In this study, the same principle was applied to recently published experimental radiotracer thermal diffusivity coefficients for all core elements in CoCrFeNiMn [42,43]. As shown in Fig. 3, $d_{Mn}/d_{Co} > d_{Cr}/d_{Co} > d_{Fe}/d_{Co} > d_{Ni}/d_{Co} > 1$ over the relevant thermal temperatures. Therefore, the fastest vacancy diffuser, Mn, should deplete while the slowest vacancy diffuser, Co, should enrich under irradiation conditions. The three elements between the fastest and slowest elements also show a corroborating trend: minimal or small depletion in Cr and Fe (second and third fast vacancy diffuser) and Ni enrichment (second slowest vacancy diffuser). The HEA vacancy diffusivities trends agree with the proposed preferential vacancy-solute mechanism similar to the Perks and MIK models in Fe-Ni-Cr austenitic stainless steels. Importantly, while the thermal vacancy diffusivity ratios can be used to indicate the direction of segregation (i.e. elemental enrichment or depletion at the GB), significant additional effort is still needed to validate this proposed vacancy dominated RIS mechanism in CoCrFeNiMn. It should also be noted that inclusion of interstitial binding effects, in similar fashion to austenitic stainless steels, could provide even better ability to predict the magnitude and level of RIS at GBs in this and other HEA alloys.

The high level of GB segregation observed, specifically the Mn depletion and Co and Ni enrichment, raises further questions to the effectiveness to reduce diffusion-controlled phenomena in chemically complex HEA alloys. Under irradiation, a situation far from thermal equilibrium with enhanced vacancy and interstitial diffusion, the segregation magnitude levels are consistent with Fe-Ni-Cr austenitic alloys. Fig. 4 shows the relative change in concentration from the GB to matrix composition for different stainless steels [44], model fcc Fe-Ni-Cr ternary alloys [34], and model fcc Ni-Cr binary alloys [34,40] in comparison to the CoCrFeNiMn examined in our study. It is observed that the magnitude of Mn depletion, the fastest diffusive species, is similar or higher in magnitude than Cr depletion, the fastest vacancy diffusive species in Fe-Ni-Cr and other model and commercial austenitic systems. The same trend in magnitude is observed for elements enriched at the GB between the austenitic stainless steels and the HEA. This is an indication that while CoCrFeNiMn may have other unique property improvements, the solid solution chemical complexity does not manifest as a minimization of RIS. This is consistent with recent bulk radiotracer diffusion studies [42,43] which has indicated that a decrease in diffusivities is not observed when the number of components increases (e.g., from CoCrFeNi to CoCrFeNiMn). Furthermore, a generalized increase in the number of elements in HEAs does not necessarily lead to enhanced sluggish diffusion. This trend is also observed in the dislocation RIS study by He et al. [18] where the magnitude of RIS to Frank loops increases from a four component system (CoCrFeNi) to a five component system (CoCrFeNiMn). The addition of core elements into HEAs and similar alloys must therefore be for a specific improvement and

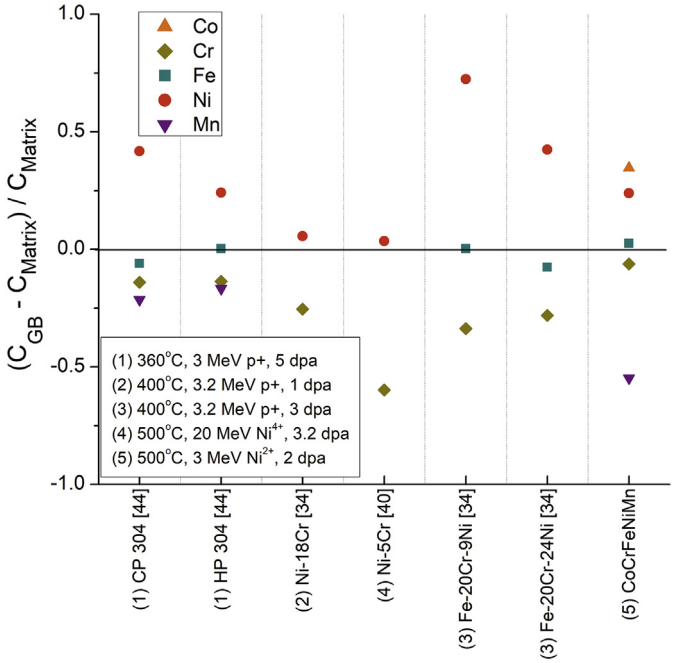

Fig. 4. Comparison in the relative change in GB to matrix composition of various fcc based single core element alloys (304 high and commercial purity [44], model Ni-Cr alloys [34,40], model Fe-Ni-Cr alloys [34]) to CoCrFeNiMn at 2 dpa; the magnitude of segregation is similar or greater in the HEA than the single core element alloys.

balance of properties. While the addition of one element may reduce sluggish diffusion, it could also play a critical role in mechanical properties (i.e. intrinsic change in stacking fault energy or low temperature twinning induced plasticity). Therefore, a balance of tailored properties with specific elements and alloy selection is critical as HEAs attempt to find commercialized value.

It was previously reported that chemical complexity under irradiation can lead to sluggish diffusion [45], reduced mobility of point defects [46] and an overall suppression of damage accumulation [16] during collision cascades. Specifically, enhanced radiation associated with void suppression by two orders of magnitude was reported in HEA alloys of CoCrFeNi and CoCrFeNiMn in comparison to Ni [22]. The suppression of voids was attributed to enhanced and localized interstitial cluster migration and subsequent point defect recombination. In agreement, our STEM-ADF shown in Fig. 1c indicates this enhanced radiation tolerance and suppression of voids (albeit at a low dose condition). While suppression of voids is critical for radiation tolerance, our study indicates that GB solute segregation in HEAs is significant and on the same level of segregation magnitude as conventional Fe-Ni-Cr alloys. It would be of interest, based on minimal RIS reduction observed in our study, to compare the reported improvements in irradiation response, specifically void swelling, dislocation size and density in multi-component HEAs to conventional alloys that have a high degree of alloying such as conventional and modified 304 and 316 type austenitic stainless steels.

In summary, we report the first observation of GB RIS behavior in the most commonly studied CoCrFeNiMn HEA. Significant depletion of Mn and enrichment of Co and Ni was observed along all RHAGBs at both 2 and 3 dpa after 500 °C 3 MeV Ni^{2+} irradiations. The segregation of Mn, Co and Ni is on the same magnitude of segregation as conventional Fe-Ni-Cr alloys under irradiation. Furthermore, the study proposes that the GB RIS mechanism follows similar trends to Fe-Ni-Cr alloys with a preferential vacancy-solute based inverse Kirkendall effect mechanism. Self-diffusion radiotracer diffusion coefficients at high temperature [42] support the vacancy dominated inverse Kirkendall mechanism of the fastest (Mn) and slowest (Co) diffuser depleting and enriching respectively at GBs.

Supplementary data to this article can be found online at https://doi.org/10.1016/j.scriptamat.2018.06.041.

Acknowledgements

C.M.B, J.E.N, and M.L.T acknowledge funding in part from the US National Science Foundation under contract 1429661 (supporting TEM instrumentation) and contract 1105681 (supporting C.M.B), and in part from the US Department of Energy, Office of Basic Energy Sciences under contract DE-SC0008274 (supporting J.E.N). This work was performed, in part, at the Center for Integrated Nanotechnologies, an Office of Science User Facility operated for the U.S. Department of Energy (DOE) Office of Science. Los Alamos National Laboratory, an affirmative action equal opportunity employer, is operated by Los Alamos National Security, LLC, for the National Nuclear Security Administration of the U.S. DOE under contract DE-AC52-06NA25396. Y. Zhang acknowledges the support of the National Natural Science Foundation of China (No. 50471025 and No. 51470124). The STEM-EDS microscopy was supported by the Center for Nanophase Materials Sciences, which is a DOE Office of Science User Facility and by using instrumentation (FEI Talos F200X S/TEM) provided by the Department of Energy, Office of Nuclear Energy, Fuel Cycle R&D Program and the Nuclear Science User Facilities.

References

[1] D.B. Miracle, O.N. Senkov, Acta Mater. 122 (2017) 448–511.
[2] Y. Zhang, T. Zuo, Z. Tang, M.C. Gao, K.A. Dahmen, P.K. Liaw, Z.P. Lu, Prog. Mater. Sci. 61 (2014) 1–93.
[3] K.E. Nygren, K.M. Bertsch, S. Wang, H. Bei, A. Nagao, I.M. Robertson, Curr. Opin. Solid State Mater. Sci. 22 (2017) 1–7.
[4] H.Y. Diao, R. Feng, K.A. Dahmen, P.K. Liaw, Curr. Opin. Solid State Mater. Sci. 21 (2017) 252–266.
[5] B. Gludovatz, A. Hohenwarter, D. Catoor, E.H. Chang, E.P. George, R.O. Ritchie, Science 345 (2014) 1153–1158.
[6] F. Otto, A. Dlouhy, C. Somsen, H. Bei, G. Eggeler, E.P. George, Acta Mater. 61 (2013) 5743–5755.
[7] M.J. Yao, K.G. Pradeep, C.C. Tasan, D. Raabe, Scr. Mater. 72–73 (2014) 5–8.
[8] C.P. Lee, C.C. Chang, Y.Y. Chen, J.W. Yeh, H.C. Shih, Corros. Sci. 50 (2008) 2053–2060.
[9] J.M. Wu, S.J. Lin, J.W. Yeh, S.K. Chen, Y.S. Huang, H.C. Chen, Wear 261 (2006) 513–519.
[10] K. Jin, C. Lu, L.M. Wang, J. Qu, W.J. Weber, Y. Zhang, H. Bei, Scr. Mater. 119 (2016) 65–70.
[11] S. Xia, M.C. Gao, T. Yang, P.K. Liaw, Y. Zhang, J. Nucl. Mater. 480 (2016) 100–108.
[12] M.-R. He, S. Wang, K. Jin, H. Bei, K. Yasuda, S. Matsumura, K. Higashida, I.M. Robertson, Scr. Mater. 125 (2016) 5–9.
[13] M.W. Ullah, D.S. Aidhy, Y. Zhang, W.J. Weber, Acta Mater. 109 (2016) 17–22.
[14] C. Lu, K. Jin, L.K. Béland, F. Zhang, T. Yang, L. Qiao, Y. Zhang, H. Bei, H.M. Christen, R.E. Stoller, L. Wang, Sci. Rep. 6 (2016), 19994. .
[15] D.S. Aidhy, C. Lu, K. Jin, H. Bei, Y. Zhang, L. Wang, W.J. Weber, Acta Mater. 99 (2015) 69–76.
[16] Y. Zhang, G.M. Stocks, K. Jin, C. Lu, H. Bei, B.C. Sales, L. Wang, L.K. Béland, R.E. Stoller, G.D. Samolyuk, M. Caro, A. Caro, W.J. Weber, Nat. Commun. 6 (2015) 8736.
[17] C. Lu, T. Yang, K. Jin, N. Gao, P. Xiu, Y. Zhang, F. Gao, H. Bei, W.J. Weber, K. Sun, Y. Dong, L. Wang, Acta Mater. 127 (2017) 98–107.
[18] M.R. He, S. Wang, S. Shi, K. Jin, H. Bei, K. Yasuda, S. Matsumura, K. Higashida, I.M. Robertson, Acta Mater. 126 (2017) 182–193.
[19] M.R. He, D.C. Johnson, G.S. Was, I.M. Robertson, Acta Mater. 138 (2017) 61–71.
[20] R.E. Stoller, M.B. Toloczko, G.S. Was, A.G. Certain, S. Dwaraknath, F.A. Garner, Nucl. Instrum. Methods Phys. Res. Sect. B Beam Interact. With Mater. Atoms 310 (2013) 75–80.
[21] M.L. Taheri, J.T. Sebastian, B.W. Reed, D.N. Seidman, A.D. Rollett, Ultramicroscopy 110 (2010) 278–284.
[22] C. Lu, L. Niu, N. Chen, K. Jin, T. Yang, P. Xiu, Y. Zhang, F. Gao, H. Bei, S. Shi, M.R. He, I.M. Robertson, W.J. Weber, L. Wang, Nat. Commun. 7 (2016) 1–8.
[23] N.A.P.K. Kumar, C. Li, K.J. Leonard, H. Bei, S.J. Zinkle, Acta Mater. 113 (2016) 230–244.
[24] T. Yang, C. Lu, K. Jin, M.L. Crespillo, Y. Zhang, H. Bei, L. Wang, J. Nucl. Mater. 488 (2017) 328–337.
[25] S.A. Briggs, C.M. Barr, J. Pakarinen, M. Mahmivand, D.D. Morgan, M.L. Taheri, K. Sridharan, J. Nucl. Mater. 479 (2016) 48–58.
[26] F.A. Garner, J. Nucl. Mater. 117 (1983) 177–197.
[27] C.M. Barr, G.A. Vetterick, K.A. Unocic, K. Hattar, X.M. Bai, M.L. Taheri, Acta Mater. 67 (2014) 145–155.
[28] G. Was, T. Allen, J. Busby, J. Gan, D. Damcott, D. Carter, M. Atzmon, E. Kenik, J. Nucl. Mater. 270 (1999) 96–114.
[29] K.G. Field, L.M. Barnard, C.M. Parish, J.T. Busby, D. Morgan, T.R. Allen, J. Nucl. Mater. 435 (2013) 172–180.
[30] J.P. Wharry, G.S. Was, J. Nucl. Mater. 442 (2013) 7–16.
[31] H. Wiedersich, P.R. Okamoto, N.Q. Lam, J. Nucl. Mater. 83 (1979) 98–108.

[32] A. Etienne, B. Radiguet, N.J. Cunningham, G.R. Odette, P. Pareige, J. Nucl. Mater. 406 (2010) 244–250.
[33] T.R. Allen, G.S. Was, Acta Metall. 46 (1998) 3679–3691.
[34] T. Allen, J. Busby, G. Was, E. Kenik, J. Nucl. Mater. 255 (1998) 44–58.
[35] J.M. Perks, A.D. Marwick, C.A. English, A Computer Code to Calculate Radiation-induced Segregation in Concentrated Ternary Alloys, AERE-R-12121, 1986.
[36] Y. Yang, K.G. Field, T.R. Allen, J.T. Busby, J. Nucl. Mater. 473 (2016) 35–53.
[37] J.P. Wharry, G.S. Was, J. Nucl. Mater. 442 (2013) 7–16.
[38] L. Barnard, J.D. Tucker, S. Choudhury, T.R. Allen, D. Morgan, J. Nucl. Mater. 425 (2012) 8–15.
[39] L. Barnard, D. Morgan, J. Nucl. Mater. 449 (2014) 225–233.
[40] C.M. Barr, L. Barnard, J.E. Nathaniel, K. Hattar, K.A. Unocic, I. Szlurfarska, D. Morgan, M.L. Taheri, J. Mater. Res. 30 (2015) 1290–1299.
[41] S.J. Rothman, L.J. Nowicki, G.E. Murch, J. Phys. F Met. Phys. 10 (1980) 383–398.
[42] M. Vaidya, K.G. Pradeep, B.S. Murty, G. Wilde, S.V. Divinski, Acta Mater. 146 (2018) 211–224.
[43] M. Vaidya, S. Trubel, B.S. Murty, G. Wilde, S.V. Divinski, J. Alloys Compd. 688 (2016) 994–1001.
[44] Z. Jiao, G.S. Was, Acta Mater. 59 (2011) 1220–1238.
[45] S. Zhao, Y. Osetsky, Y. Zhang, Acta Mater. 128 (2017) 391–399.
[46] Y.N. Osetsky, L.K. Béland, R.E. Stoller, Acta Mater. 115 (2016) 364–371.